Journal of Information Hiding and Multimedia Signal Processing ©2021 ISSN 2073-4212
Ubiquitous International Volume **12**, Number **1**, March **2021**

Numerical Analysis of Dispersion Characteristics of a Photonic Crystal Fiber

Ibrahima Djenabou Barry

Graduate School of Agriculture and Engineering
University of Miyazaki
Gakuenkibanadai Nishi 1-1 889-2192 Miyazaki, Japan
barryibrahima427@gmail.com

Mitsuhiro Yokota

Department of Electrical and Systems Engineering
University of Miyazaki
Gakuenkibanadai Nishi 1-1 889-2192 Miyazaki, Japan
t0b210u@cc.miyazaki-u.ac.jp

Received September 2020; revised November 2020

Abstract. *In this manuscript, we numerically examined the dispersion characteristics of two designed microstructure fibers by using the plane wave expansion method. In the basic structure, air holes are arranged in a square lattice. In the first structure, the third ring in the cladding is formed by small diameter circular air-holes. In the second fiber, the third ring is formed by large diameter circular air-holes and in both fibers, the first ring around the germanium doped core is formed by elliptical air-holes filled with ethanol. By manipulating the third ring air-holes diameter, we obtained flat negative dispersion or dispersion compensation property. Additionally, we compared the dispersion diagrams of the small third ring air-holes diameter fiber with the large third ring air-holes diameter fiber.*
Keywords: Photonic crystal fiber, dispersion diagram, flat negative dispersion, plane wave expansion (PWE) method.

1. Introduction.

The invention of the photonic crystal fiber has solved one of the greatest difficulties encountered in the field of telecommunication, which is the control of the dispersion in fibers. The dispersion diagram is one of the most important properties of a waveguiding medium. With the flexibility of its cladding, formed with air-holes, it is possible to obtain different dispersion properties like dispersion compensation, flattened or ultra-flattened dispersion, zero-dispersion, and so on. The dispersion compensating fiber can be realized with square lattice fiber with a small pitch and a large diameter air-holes [1]. Also, a square lattice with an elliptical designed core with small pitch values and large air-holes can give a dispersion compensation property [2]. In reference [3], they studied, the influences of elliptical holes on the dispersion by introducing one or more rings of elliptical air-holes and obtained ultra-low and ultra-flattened dispersion photonic crystal fiber. To investigate the properties of light propagating in a photonic waveguide usually, the Computational Photonics method is used that is seen as the substitution to the expensive experimental equipment. As computational methods are categorized as follows:

frequency-domain eigensolvers, frequency-domain solvers, and time-domain simulations. Among the computational methods are BPM (Beam propagation method), EME (Eigen-mode Expansion Methods), FDTD (Finite Difference Time Domain) method [4, 5]. In reference [6], an algorithm based on the method of line (MoL) is used to numerically analyze a holey fiber. In our simulation, the Plane Wave Expansion (PWE) is used as the simulation method to compute the dispersion characteristics of the fiber [7].
In this paper, we numerically examined the dispersion characteristics of two (2) designed photonic crystal fibers consisting of six (6) rings of holes in the cladding area. In the first fiber, the third ring in the cladding is formed by a small diameter of air-holes, and the first ring around the germanium doped core is formed by elliptical air-holes filled with ethanol. In the second proposed fiber, the third ring in the cladding area is formed by large diameter air-holes, and the first ring around the germanium doped core is formed by elliptical air-holes filled with ethanol. By manipulating the diameter of the air-holes of the third ring we obtained a flat negative dispersion or a dispersion compensation property. Additionally, we also compared the dispersion diagram of the small third ring air-holes diameter with the dispersion diagram of the large third ring air-holes diameter of the fibers. The plane wave expansion (PWE) is used as the simulation method.

2. **Numerical Analysis of the proposed fibers.**

2.1. **Cross-section of the proposed fibers.**

The below Fig.1 is the cross-section of the two designed solid-core fibers with six (6) rings of holes surrounding the core; the first rings of both fibers are formed with elliptical air-holes filled with ethanol. a, b and η represent, respectively the major axis, the minor axis, and the ellipticity of the fiber. d_1 is the diameter of the third ring air-holes with a radius r_1. d is the diameter of the remaining circular air-holes in the cladding area of both fibers with a radius of $r = 0.25\Lambda$. Λ represents the pitch or the distance center to center of two nearest air-holes. The core of the designed fibers is doped with germanium and defined as d_c=2Λ - d.

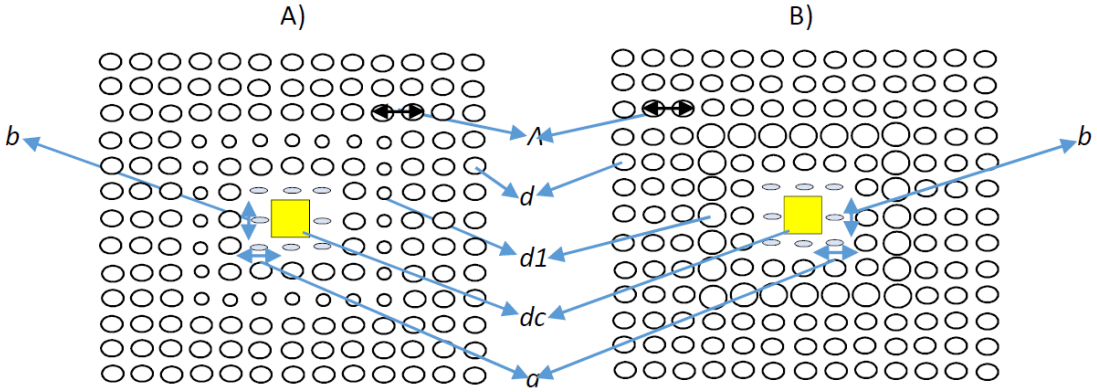

FIGURE 1. Cross-section of the two proposed Square Lattice Photonic Crystal Fibers. A) Square lattice photonic crystal fiber with small third ring air-holes with a radius r_1=0.15Λ. B) Square lattice photonic crystal fiber with large third ring air-holes with a radius r_1=0.5Λ.

3. **Theory.**

Knowing that the plane wave expansion method is known to be one of the most favorable methods when dealing with a periodic structure for the analysis of the properties or more specifically the dispersion of a photonic crystal fiber [7, 8, 9]. The general idea in a brief form of the plane wave expansion method [10]. Maxwell's equation after taking out the electric field from time-harmonic the following is obtained:

$$\nabla \times (\frac{1}{n^2}\nabla \times \mathbf{H}) = \kappa^2 \mathbf{H} \tag{1}$$

$$\nabla \cdot \mathbf{H} = 0 \tag{2}$$

Where H is the magnetic field, κ represents the wavenumber and n is the refractive index. The changes of the refractive index in the z-direction and expanding the H as expressed as follows, to find the Eigen-states:

$$\mathbf{H}(x, y, z) = \mathbf{h}(x, y)\, e^{i\beta z} = (\mathbf{h}_t(x, y) + h_z(x, y)\overrightarrow{\mathbf{z}})e^{i\beta z} \tag{3}$$

Where, β is the propagation constant.

The calculation of the dispersion in the proposed fiber is done by Eq. (4), where λ is the wavelength in free space, c the speed of light in a vacuum, and n_{eff} represent the effective refractive index in the fiber. Eq. (5) determines the effective refractive index, and the propagation constant β is calculated numerically with the plane wave expansion method as shown in the dispersion diagrams of Fig. 2 and Fig. 8 and also, κ_0 is the wavenumber in free space which is calculated by Eq. (6).

$$D(\lambda) = -\frac{\lambda}{c}\frac{d^2 n_{eff}}{d\lambda^2} \tag{4}$$

$$n_{eff} = \frac{\beta}{\kappa_0} \tag{5}$$

$$\kappa_0 = \frac{2\pi}{\lambda} \tag{6}$$

4. **Dispersion Characteristics of the fibers.**

4.1. **Calculation of the dispersion diagram of the fibers.**

4.1.1. *Square lattice photonic crystal fiber with small third ring air-holes diameter ($r_1 = 0.15\Lambda$).*

The proposed fibers are solid-core fibers. It is well known that the solid core photonic crystal fiber guides light by total internal refraction (TIR) different from the bandgap fiber, which guides light by a photonic bandgap in the cladding area.

The below Fig. 2, shows the dispersion diagram of the designed fiber with a small third ring air-hole diameter. The first part (Red) is the continuum of states with a range of frequencies and propagation constants. The presence of one large opened bandgap and other small ones in the cladding area of our proposed fiber. The third ring air-hole's radius is defined as r_1=0.15Λ and (d_1/Λ) =0.3 with a pitch value of Λ=2.07µm. The radius of the remaining circular air-holes is determined as $r = 0.25\Lambda$. The major and minor axis of the elliptical holes are also determined as a=1.2 µm and b=0.5 µm respectively, the ellipticity is η=2.4. a, b and η are constant values in our simulation. The region below the continuum of state (cladding) is the defect Eigen-state represented by the core area of the fiber. The region in between the defect Eigen state and the continuum states

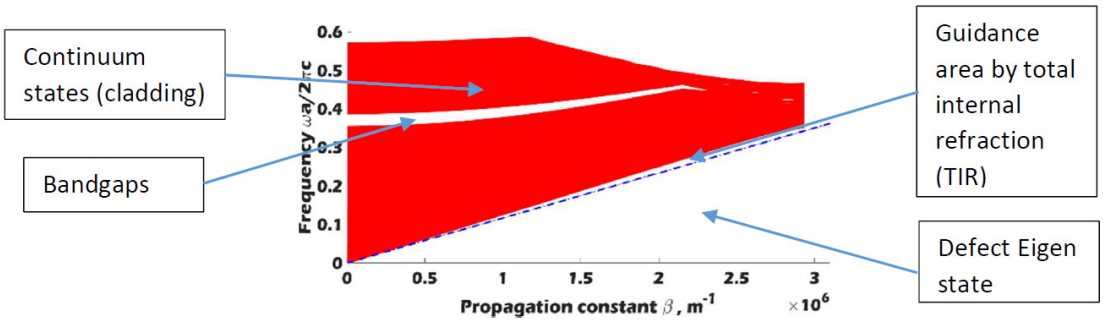

FIGURE 2. Dispersion diagram of the fiber. The continuum of states (Red part) and the defect Eigen states below the continuum states (cladding area) of the solid core square lattice photonic crystal fiber with small third ring air-hole diameter (r_1=0.15Λ), (d_1/Λ) =0.3.

(cladding area) is the guidance area, where light is guided by total internal refraction (TIR). This indicates that light propagating in this range of frequencies and propagation constants, will not enter the cladding area of the proposed fiber rather will propagate in the core area. By choosing the right range of frequencies and propagation constants in the guidance area, we can determine the effective refractive index as indicated in Eq. (5). Therefore, for the calculation of the effective indices, we used the plane wave expansion method [10, 11, 12].

4.2. **Distribution of the reciprocals refractive index in the cross-section of the Square Lattice Photonic Crystal Fiber with small third ring air-holes diameter (r_1=0.15Λ).**

In Fig. 3, the distribution of the refractive index in the cross-section is as follows, the distribution of the refractive index of the background (blue area) is $n = 1.45$, the cladding composed with air-holes of refractive index $n_{cl} = 1$ (red circles). The first ring around the core is formed with elliptical air-holes filled with ethanol of refractive index n_{eth}=1.3611; the core area is doped with germanium of a doping concentration of 19.3%.

4.3. **Field distribution in the Square Lattice Photonic Crystal Fiber with small third ring air-holes diameter ($r_1 = 0.15\Lambda$).**

In Fig. 4, the first eigenvector which coincides with the first eigenstate calculated in the dispersion diagram in Fig. 2 of the photonic crystal fiber is used for the computation of the fundamental mode of the fiber; as it can be seen as a confined light in the doped core area. Strong guidance in the fiber is observed.

In Fig. 5, the effective refractive index is determined by the numerically calculated propagation constant β of the dispersion diagram in Fig. 2, of the fiber with small third ring air-holes. For a normalized interval of frequencies in the guidance region from 0.185 to 0.352 the light propagating in this range, propagates in the doped solid-core of the proposed fiber with small third ring air-holes, justifying the obtained effective refractive index in Fig. 5. After numerically calculating the effective refractive index, Eq. (4) is then used to determine the dispersion characteristics as shown below in Fig. 6.

Knowing that dispersion can be controlled within a wide range of wavelengths by varying the diameter of air-holes and pitch values in the cladding area [14, 15, 16]. The

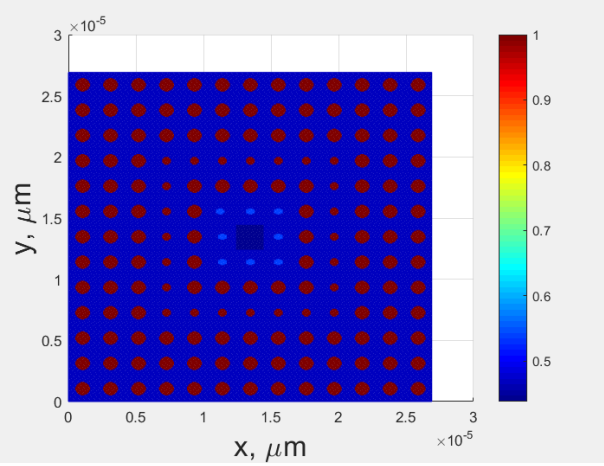

FIGURE 3. The distribution of the reciprocals of the refractive index in the cross-section of the Square lattice photonic crystal fiber with small third ring air-holes diameter r_1=0.15Λ, Λ=2.07µm, d_1=0.621 µm, and d=Λ/2.

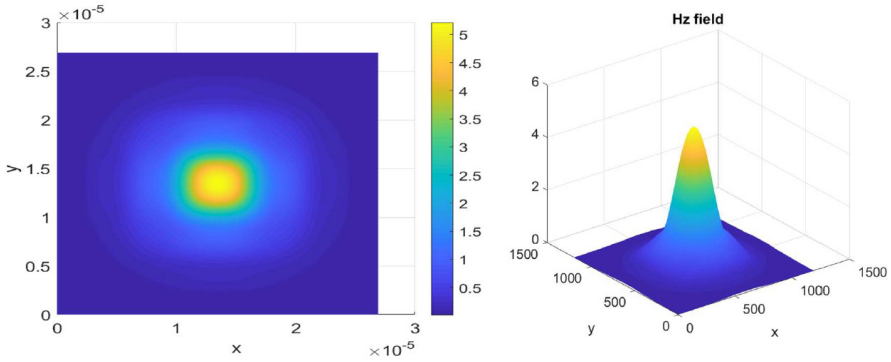

FIGURE 4. Field distribution in the Square Lattice Photonic Crystal Fiber representing the fundamental mode with small third ring air-holes diameter, $r_1 = 0.15\Lambda$, d_1 =0.621µm, d =Λ/2, Λ=2.07µm.

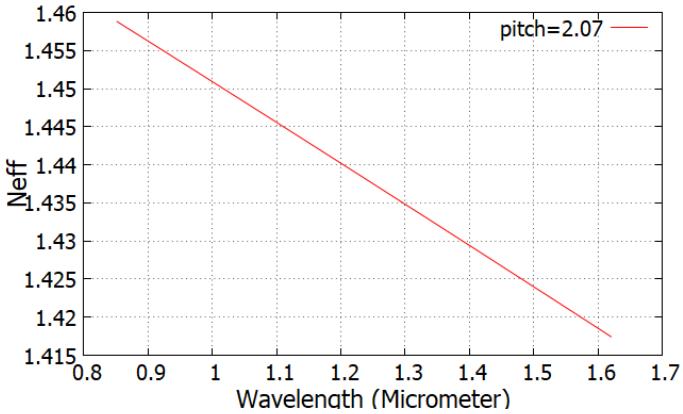

FIGURE 5. The effective refractive index of the Square Lattice Photonic Crystal Fiber with small third ring air-hole diameter (r_1 = 0.15Λ), d=Λ/2=1.035µm, d_1 = 0.621 µm, and Λ=2.07µm

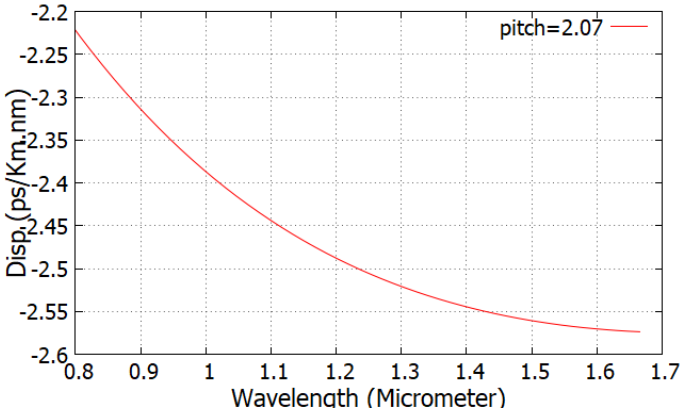

FIGURE 6. Dispersion of the design Square Lattice Photonic Crystal Fiber with small third ring air-hole diameter ($r_1 = 0.15\Lambda$). With Λ=2.07µm, d=$\Lambda/2$ and $d_1 = 0.621$ µm, $(d_1/\Lambda) = 0.3$

dispersion curve in Fig. 6, gave negative values in a large range of wavelengths. We obtained a flat negative dispersion. Additionally, the dispersion coefficient in the fiber shift from greater values to smaller ones as the wavelength continues to increase or we can say that the dispersion decreases as the wavelength increases. Because of the negativity of its dispersion, the designed fiber can find its application in the wide group of dispersion compensation fibers. In the following Fig. 7, by varying the pitch of the microstructure fiber with small third ring air-holes for Λ=2.07, 2.1, and 2.13µm, it creates a change into the dispersion of the fiber as it can be seen, the negativity of the dispersion increased in the range of -2.2 to -3.1 (ps/Km. nm). Also, by reducing the pitch Λ of the fiber from 2.13 µm to 2.07 µm we observed that the curve of the dispersion becomes flatter.

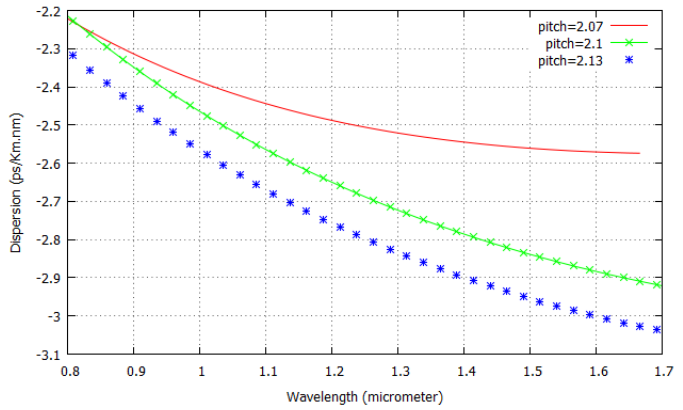

FIGURE 7. Effect of the pitch on the dispersion of the Square Lattice Photonic Crystal Fiber with small third ring air-hole diameter ($r_1 = 0.15\Lambda$) and Λ=2.07, 2.1, 2.13µm

4.4. **Square Lattice Photonic Crystal Fiber with large third ring air-holes diameter ($r_1 = 0.5\Lambda$).**

The dispersion diagram has been deeply explained in Fig. 2 when the third ring air-holes diameter had a radius of r_1=0.15Λ and a diameter d_1=0.621 µm less than the pitch of the fiber Λ=2.07 µm. In Fig. 8, by increasing the diameter of the third ring to a value equal

to the pitch of the fiber d_1=Λ =2.07µm for a radius of r_1=0.5Λ. We observed that more bandgaps opened in the continuum state or in the cladding area. Because of increasing the ratio from d_1/Λ =0.3 to d_1/Λ=1.0, a different dispersion diagram is obtained with more open bandgaps in the cladding area.

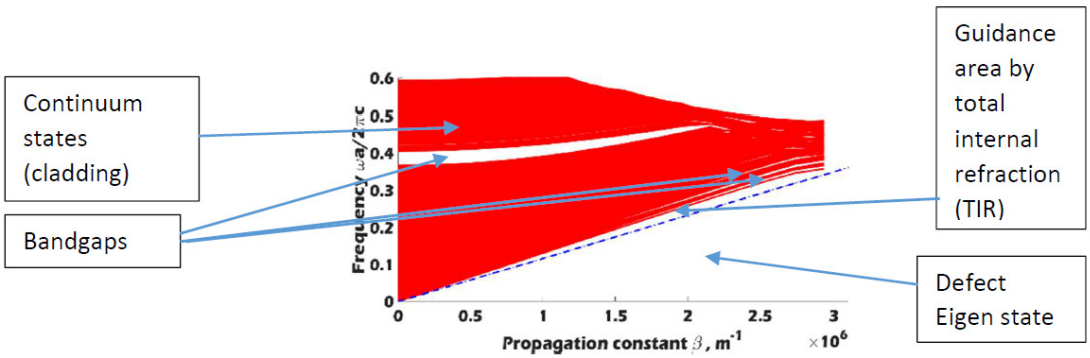

FIGURE 8. The dispersion diagram of the fiber. The continuum of states (Red part) and the defect Eigen states below the continuum states (cladding area) of the solid core square lattice photonic crystal fiber with large third ring air-hole diameter (r_1 = 0.5Λ), d_1 =Λ=2.07µm, d=Λ/2.

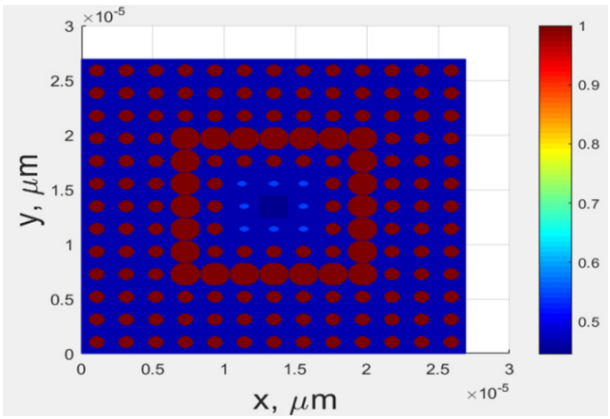

FIGURE 9. The distribution of the reciprocals of the refractive index in the cross-section of the Square lattice photonic crystal fiber with large third ring air-holes diameter r_1=0.5Λ, d=Λ/2, d_1=Λ=2.07µm, (d_1/Λ) =1.0

By manipulating or varying the diameter of the air-holes in the third ring of the designed square lattice photonic crystal fiber with large third ring air-holes diameter. In Fig. 9, the distribution of the refractive index in the cross-section with a large third ring air-holes diameter of a radius r_1=0.5Λ and a pitch value of Λ=2.07µm is shown. In Fig. 10, the propagated light becomes more confined, and strong guidance on the doped solid core is observed. The fundamental mode is determined with the first eigenvector which coincides with the first eigenstate numerically calculated in the dispersion diagram in Fig. 8.

In Fig.11, with the numerically calculated propagation constant β of the dispersion diagram, in Fig. 8, the effective refractive index of the solid-core fiber with large third ring air-holes diameter is calculated and compared with the effective refractive index of the fiber with small third ring air-holes diameter. As it is shown in Fig. 11, by increasing the

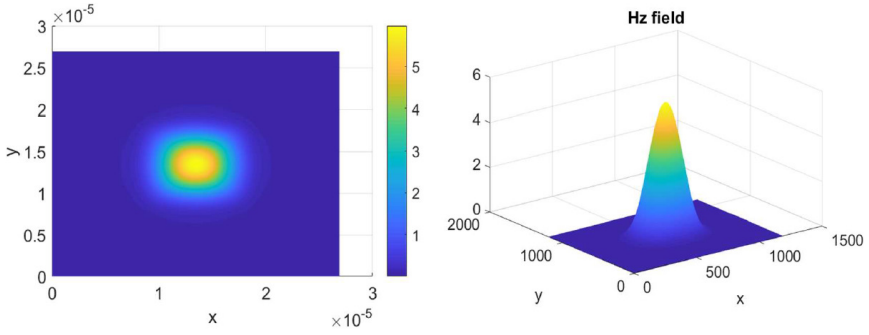

FIGURE 10. Field distribution in the Square Lattice Photonic Crystal Fiber representing the fundamental mode with large third ring air-holes diameter, r_1=0.5Λ, d=Λ/2, d_1=Λ=2.07µm, (d_1/Λ) =1.0

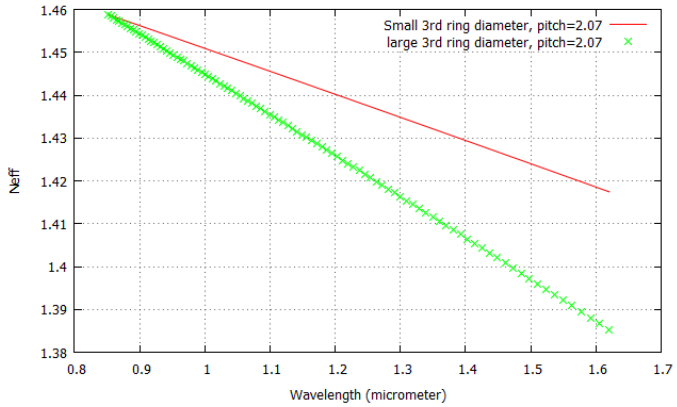

FIGURE 11. Effective refractive index of both doped solid core Photonic Crystal Fibers with small and large third ring air-hole diameter ($r_1 = 0.15\Lambda$ and $r_1 = 0.5\Lambda$), d=Λ/2 and Λ=2.07µm

diameter of the air-holes of the third ring the effective refractive index decreases causing the opening of more bandgaps in the cladding area.

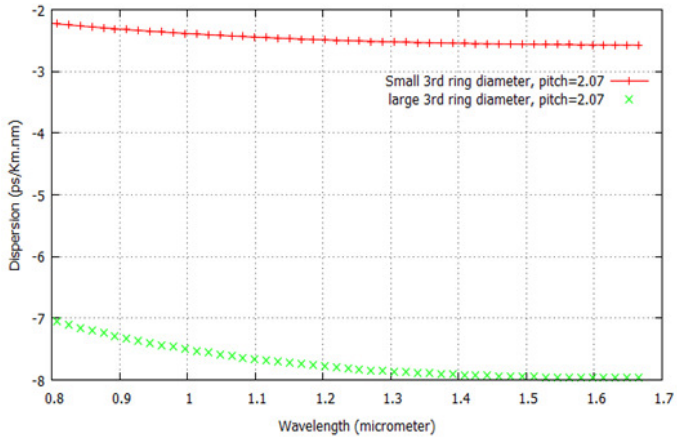

FIGURE 12. The dispersion characteristics of both doped solid core Photonic Crystal Fibers with small and large third ring air-hole diameter ($r_1 = 0.15\Lambda$ and $r_1 = 0.5\Lambda$) with d=Λ/2, Λ=2.07µm

From the obtained values of the effective indices, we compared the dispersion of both photonic crystal fibers in Fig. 12. By increasing the size of the air-holes diameters in a photonic crystal fiber it is possible to realize a large dispersion in a large range of wavelength [16]. With the increase of the diameter or the radius of the third ring air-holes to r_1=0.5Λ, the negativity also becomes important and a flat dispersion is also obtained. We can conclude that the variation of the diameter of the third ring circular air-holes affects the dispersion characteristics in the fibers. In table 1, we compared the dispersion of both photonic crystal fibers at different wavelengths. The negativity in the fiber increases with the increase of the wavelengths.
Additionally, we can see from table 1, with the increase of the radius to a value of r_1=0.5Λ the dispersion of the fiber becomes negatively significant and the dispersion coefficient is almost multiplied three times.

Table 1. Comparison of the Dispersion in both PCFs

Wavelengths (µm)	Dispersion of the small third ring diameter PCF (ps/km.nm) $r_1 = 0.15\Lambda$	Dispersion of the large third ring diameter PCF (ps/km.nm) $r_1 = 0.5\Lambda$
0.5	-1.417737357	-4.583019771
0.8	-1.878423549	-6.009486388
1.3	-2.308148558	-7.325023434
1.55	-2.415784527	-7.587149158
2.0	-2.539242733	-7.905263308

5. **Conclusions.**

In this paper, the dispersion characteristics of two (2) designed square lattice photonic crystal fibers with six (6) rings of holes around a germanium doped core, has been carefully investigated. For the fiber with small third ring air-holes diameter and a radius r_1=0.15Λ, a dispersion diagram of one large opened bandgap in the cladding area and a flat negative dispersion curve is obtained. Additionally, by reducing the pitch, the dispersion becomes flatter in the fiber. For the fiber with a large third ring diameter and a radius r_1=0.5Λ, we observed more opening bandgaps in the cladding area and the dispersion curve is also flat. The negativity of the dispersion becomes more important and almost three times larger. By comparing the dispersion diagrams of both fibers, the increment of the diameter of the third ring air-holes causes the effective refractive index to decrease, and the opening of more bandgaps in the cladding area. It is also observed that the light is more confined in the fiber with large third ring air-holes than the one with small third ring air-holes. The designed fibers can find their applications in the wide group of dispersion compensated fibers.

REFERENCES

[1] A. H. Book, A. Cucinotta, F. Poli, S. Selleri, Dispersion properties of square-lattice photonic crystal fibers, *Opt. Society of Am.*, vol. 12, pp. 941-946, 2004.
[2] P. S. Maji, Partha, R. Chaudhuri, Dispersion properties of the square-lattice elliptical core PCFs, *American J. of Optics & Photonics*, vol. 1, pp. 1-6, 2014.
[3] J. Wang, C. Jiang, W. Hu, M. Gao, H. Ren, Dispersion and polarization properties of elliptical air-hole-containing photonic crystal fibers, *Opt.& laser Tech.*, vol.39, pp. 913-917, 2007.

[4] M. S. Wartak, *Computational photonics an introduction with matlab*, Cambridge University Press, New Y., pp.2-3, 2013.
[5] J. D. Joannopoulos, S. G. Johnson, J. N. Winn, and R. D. Meade, *Photonic crystals: Modeling the flow of light*, Princeton University Press, Princeton and Oxford, 2008.
[6] Igor A. Goncharenko, Stefan F. H., Reinhold P., Radiation loss and mode field distribution in curved holey fibers, *Int. J. Electron. Commun. (AEU)*, vol.59, pp.185-191, 2005.
[7] J. Wang, C. Jiang, W. Hu, M. Gao, Modified design of photonic crystal fibers with flattened dispersion, *Optics & laser Techn.*, vol. 38, pp.169-172, 2006.
[8] Bjarklev A, Broeng J, Bjarklev As, *Photonic crystal fibers*, Dordrecht, kluwer Academic Publishers, 2003.
[9] Knight JC, Birks TA, Russell PSJ, Atkin DM, All-silica single mode optical fiber with photonic crystal cladding, *Opt. Lett.*, vol.21, pp.1547-1549, 1996.
[10] H. Demir, S. Ozsoy, Large-solid-core square-lattice photonic crystal fiber, *Opt. Fiber Techn.*, vol.17, pp.594-600, 2011.
[11] Rsoft design group
[12] J. Arriaga, J.C. Knight, P. St. J. Russell, modeling photonic crystal fibers, *Physica E.*, vol. 17, pp. 440-442, 2003.
[13] J. Arriaga, J. C. Knight, P. St. J. Russell, Modeling the propagation of light in photonic crystal fibers, *Physica D*, vol. 180, pp. 100-106, 2004.
[14] Pranaw K, Vikash K, J. Sekhar R, Design of quad core photonic crystal fibers with flattened zero dispersion, Int. J. Commun. (AEU), vol. 98, pp. 265-272, 2019.
[15] Beata Z, Jesper L, Anders B, A novel photonic crystal fiber design for dispersion compensation, *J. Opt. A: Pure Appl. Opt.*, vol. 6, pp. 717-720, 2004.
[16] T. A. Birks, D. Mogilevtsev, J. C Knight, P. St J. Russell, Dispersion compensation using single material fibers, *IEEE Photon Techn. Lett.*, vol. 11, pp. 674-676.